Evaluation of Coincident Passive Microwave Rainfall Estimates Using TRMM PR and Ground Measurements as References

XIN LIN* AND ARTHUR Y. HOU

Global Modeling and Assimilation Office, NASA Goddard Space Flight Center, Greenbelt, Maryland

(Manuscript received 11 October 2007, in final form 31 March 2008)

ABSTRACT

This study compares instantaneous rainfall estimates provided by the current generation of retrieval algorithms for passive microwave sensors using retrievals from the Tropical Rainfall Measuring Mission (TRMM) precipitation radar (PR) and merged surface radar and gauge measurements over the continental United States as references. The goal is to quantitatively assess surface rain retrievals from cross-track scanning microwave humidity sounders relative to those from conically scanning microwave imagers. The passive microwave sensors included in the study are three operational sounders—the Advanced Microwave Sounding Unit-B (AMSU-B) instruments on the *NOAA-15*, *-16*, and *-17* satellites—and five imagers: the TRMM Microwave Imager (TMI), the Advanced Microwave Scanning Radiometer for the Earth Observing System (AMSR-E) instrument on the *Aqua* satellite, and the Special Sensor Microwave Imager (SSM/I) instruments on the Defense Meteorological Satellite Program (DMSP) *F-13*, *-14*, and *-15* satellites. The comparisons with PR data are based on "coincident" observations, defined as instantaneous retrievals (spatially averaged to 0.25° latitude and 0.25° longitude) within a 10-min interval collected over a 20-month period from January 2005 to August 2006. Statistics of departures of these coincident retrievals from reference measurements as given by the TRMM PR or ground radar and gauges are computed as a function of rain intensity over land and oceans. Results show that over land AMSU-B sounder rain retrievals are comparable in quality to those from conically scanning radiometers for instantaneous rain rates between 1.0 and 10.0 mm h^{-1}. This result holds true for comparisons using either TRMM PR estimates over tropical land areas or merged ground radar/gauge measurements over the continental United States as the reference. Over tropical oceans, the standard deviation errors are comparable between imager and sounder retrievals for rain intensities above 5 mm h^{-1}, below which the imagers are noticeably better than the sounders; systematic biases are small for both imagers and sounders. The results of this study suggest that in planning future satellite missions for global precipitation measurement, cross-track scanning microwave humidity sounders on operational satellites may be used to augment conically scanning microwave radiometers to provide improved temporal sampling over land without degradation in the quality of precipitation estimates.

1. Introduction

Accurate measurements of the space–time distribution of precipitation are essential not only for a better understanding of the global water and energy cycle but also for improving weather, climate, and hydrological predictions. With the coverage of traditional ground-based measurements from gauges and radars concentrated over well-populated land regions, a comprehensive description of the space–time variability of global precipitation can only be achieved with observations from space.

Although infrared (IR) and visible (VIS) instruments can provide information such as cloud cover and cloud-top temperatures from which to infer precipitation rates (e.g., Kilonsky and Ramage 1976; Griffith et al. 1978; Arkin 1979; Arkin and Meisner 1987), the backbone of space-based precipitation measurements are microwave sensors that directly respond to the absorption and scattering of cloud hydrometer particles (e.g., Wilheit et al. 1977; Spencer et al. 1989; Liu and Curry 1992; Petty 1994a,b; Kummerow et al. 1996; Olson et al. 1996).

As shown in Wilheit (1986) and Spencer et al. (1989),

* Additional affiliation: Goddard Earth Sciences and Technology Center, University of Maryland, Baltimore County, Baltimore, Maryland.

Corresponding author address: Dr. Xin Lin, NASA Goddard Space Flight Center, Code 610.1 Greenbelt, MD 20771.
E-mail: xin.lin-1@nasa.gov

DOI: 10.1175/2008JAMC1893.1

© 2008 American Meteorological Society

liquid drops absorb and scatter microwave radiation, with absorption dominating the radiative transfer, whereas ice generally only scatters microwave radiation. Both scattering and absorption tend to increase with frequency and with rain rate. Based on these radiative properties, rain rates in tropical oceans can be estimated through sensing the thermal emission (and scattering) of raindrops over the radiometrically cold ocean at relatively low passive microwave (PMW) frequencies, whereas rain rates over land can be estimated from the scattering signal due to ice particles at relatively high frequencies (e.g., Wilheit et al. 1977; Spencer et al. 1983; Wilheit 1986; Spencer 1986; Grody 1991; Adler et al. 1993).

Among microwave sensors, the quality of rain retrievals varies with sensor characteristics, surface emission, and many other factors. For example, because of the low, relatively uniform ocean surface emissivity, rain rates over the tropical and subtropical oceans can be physically retrieved with good accuracy from conically scanning radiometric imager data using emission-based (or emission–scattering-combined) rainfall algorithms (e.g., Wilheit 1986; Spencer et al. 1989; Petty 1994a,b; Smith et al. 1994a,b,c; Kummerow et al. 1996; Olson et al. 1996). However, over land where the scattering-based algorithms are usually applied, rain rates are still largely empirically retrieved and have significant uncertainties. Not only is the scattering of microwave radiation highly dependent on the poorly known details of the ice-size distribution, but also the precipitation estimate is primarily related to the presence of frozen hydrometeors aloft, which have a less direct relationship with surface rain rates. Further, highly variable land surface—including different vegetation cover, snow and ice cover, and soil wetness, all of which may change significantly with time—makes it difficult to distinguish rainfall pixels from complicated surface backgrounds (e.g., Wilheit 1986; Kummerow et al. 2001; Ferraro et al. 2005). Rain retrievals from microwave sounder data may have uncertainties over land similar to those from radiometer data. On the other hand, applying algorithms based on scattering only to high-frequency microwave sounder data over tropical and subtropical oceans usually leads to biases in detecting rain events that lack ice phase processes (e.g., Joyce et al. 2004; Ferraro et al. 2005; Huffman et al. 2007). Quantitatively evaluating these satellite rainfall retrievals against the "true" rainfall distribution over both ocean and land is therefore an important and challenging task.

A major obstacle in evaluating satellite rainfall products is that there are no perfect observations to serve as the "truth." Despite well-known issues with ground-based measurements (e.g., calibration and representativeness errors), validation studies often use rain gauge and surface radar data as the reference to directly evaluate satellite rainfall retrieval algorithms (e.g., Allam et al. 1993; Smith et al. 1998; Ebert and Manton 1998; Kummerow et al. 1998, 2001; Olson et al. 2006). Although many valuable insights have been gained into the retrieval error statistics by using surface measurements to evaluate satellite rainfall estimations, a number of issues remain when using ground measurements as the reference:

(i) Evaluations of satellite rainfall retrievals against ground-based observations are typically performed over a few sites over open oceans and some well-instrumented land areas (e.g., Smith et al. 1998; Yang et al. 2006). Because the rainfall error statistics can be highly regime-dependent, there have been concerns that the error statistics derived from limited oceanic sites and land areas may not be applicable to other parts of the world (e.g., Kummerow et al. 1998; Nesbitt et al. 2004; Berg et al. 2006).

(ii) PMW sensors and their rainfall retrieval algorithms have different sensitivities on the rain/no rain detection, and rain retrieval errors may vary as a function of rain intensities. Because of the small number of raining samples resulting from limited satellite overpasses over ground validation sites, the traditional scatterplot and a single correlation number are not able to quantitatively describe the nonlinear properties of rainfall retrieval error statistics at different rain intensities (e.g., Conner and Petty 1998).

(iii) Monthly-mean or seasonal-mean comparisons are usually performed to evaluate rainfall retrievals on board different satellites at regional and global scales. Most satellites are nongeostationary, and if retrievals are not coincidently compared with a common reference, retrieval errors, random errors, and diurnal undersampling errors would all be merged in the computed statistics (e.g., Wilheit 1986; Hong et al. 1997; Lin et al. 2002), which makes it difficult to feed back the retrieval problem to the algorithm developers.

The successful operation of Tropical Rainfall Measuring Mission (TRMM; Simpson et al. 1988, 1996) has provided new and extensive space-borne observations of the hydrologic cycle in the tropics and subtropics. Of the two rain-sensing instruments flown on TRMM, the precipitation radar (PR; Meneghini and Kozu 1990; Kummerow et al. 1998, 2000; Iguchi et al. 2000) provides the first spaceborne active microwave rainfall re-

TABLE 1. Characteristics of satellites and sensors that provide microwave rainfall retrievals.

Satellite	Swath width (km)	Microwave channels	Microwave frequencies (GHz)	Rain pixel resolution (km)
TRMM PR	247	1	13.8	5
TRMM TMI	878	9	10.7, 19.4, 21.3, 37, 85.5	14
DMSP *F-13* SSM/I	1700	7	19.4, 21.3, 37, 85.5	15
DMSP *F-14* SSM/I	1700	7	19.4, 21.3, 37, 85.5	15
DMSP *F-15* SSM/I	1700	7	19.4, 21.3, 37, 85.5	15
EOS *Aqua* AMSR-E	1700	12	6.9, 10.7, 18.7, 23.8, 36.5, 89	15
NOAA-15 AMSU-B	2334	5	89–183.3	16
NOAA-16 AMSU-B	2334	5	89–183.3	16
NOAA-17 AMSU-B	2334	5	89–183.3	16

trieval, with a horizontal footprint of 5 km over a swath of 247 km (after the orbit boost in August 2001). Not only have PR data been undergoing rigorous internal and external calibrations, they have also been evaluated favorably against surface observations over different oceanic and land validation sites (e.g., Schumacher and Houze 2000; Liao et al. 2001). Considering the PR's stable and active microwave sensing features (especially its theoretical superiority to overland PMW technique), the PR data together with conventional ground-based measurements can provide independent yet mutually supplemental references for assessing other rainfall retrievals.

To guide the planning of future satellite precipitation-measuring missions, we have compared instantaneous rainfall estimates provided by several widely available operational rainfall products in the tropics and subtropics. To address some of the concerns regarding rainfall evaluation discussed in the previous section, both TRMM PR data and merged surface radar and gauge data over the continental United States are used as references to quantitatively evaluate the error statistics of surface rainfall retrievals derived from three operational sounders—the Advanced Microwave Sounding Unit-B (AMSU-B) instruments on *NOAA-15*, *-16*, and *-17* satellites—and five imagers: the TRMM Microwave Imager (TMI; Kummerow et al. 1998), the Special Sensor Microwave Imager (SSM/I) instrument on the Defense Meteorological Satellite Program (DMSP) *F-13*, *-14*, and *-15* satellites, and the Advanced Microwave Scanning Radiometer for the Earth Observing System (AMSR-E) instrument on the *Aqua* satellite.

In this study, comparisons of PMW retrievals against PR data are based on "coincident" observations, defined as instantaneous retrievals (spatially averaged to 0.25° in latitude and 0.25° in longitude) within a 10-min interval collected over a 20-month period from January 2005 to August 2006. Further coincident comparisons against surface radar and gauge data are made at 1-h intervals for a 3-month period from June to August 2005 over the continental United States south of 35°N. The goal is to quantitatively assess surface rain retrievals from cross-track scanning microwave humidity sounders relative to those from conically scanning microwave imagers. Statistics of departures of the coincident retrievals from reference measurements as given by the TRMM PR and ground radar and gauges are computed as a function of rain intensity over land and ocean.

Section 2 introduces satellite rainfall retrievals, explains how they are analyzed, and discusses the definition of coincidence and coincident samples for different sensors. Section 3 examines the rain–no rain detection in different PMW retrievals. Sections 4 and 5 present results from collocated comparisons against TRMM PR over land and ocean, focusing on quantifying retrieval error statistics for different PMW rainfall estimates. Section 6 further examines the satellite rainfall retrievals, including those from TRMM PR against ground measurements over the continental United States. Section 7 presents the final conclusions of the study and proposes some future work for further quantitative evaluations of satellite rainfall estimations.

2. Data and analysis methods

a. Satellites and sensors

PMW rainfall retrievals from eight satellites—TRMM, DMSP *F-13*, *-14*, and *-15*, *Aqua*, and three National Oceanic and Atmospheric Administration (NOAA) Polar Orbiting Environmental Satellites (*NOAA-15*, *-16*, and *-17*, respectively)—are analyzed in this study. Detailed information regarding the satellites and sensors is listed in Table 1.

The TRMM satellite was launched in November 1997 to understand the temporal and spatial distributions of precipitation and latent heating in the tropics and subtropics (Simpson et al. 1988; Kummerow et al. 1998). TRMM's orbit is circular, with an inclination angle of 35° relative to the equator. The PR and TMI are two microwave sensors on board TRMM to retrieve pre-

cipitation and latent heat release in distinctly different manners. TMI is a nine-channel passive microwave radiometer measuring radiances at five frequencies; PR is the first quantitative space-borne K_u-band weather radar operating at a frequency of 13.8 GHz. Because of their swath differences (TMI: 878 km; PR: 247 km, boosted after August 2001), TMI tends to sample a given area in the tropics and subtropics about once per day, but at a different local time every day, whereas PR visits a given area on the average of about once every 3 days.

SSM/I—one of a suite of sensors flown on the DMSP satellites—is a seven-channel, four-frequency, linearly polarized PMW radiometric system that measures upwelling microwave radiance at 19.35, 22.3, 37.0, and 85.5 GHz. The DMSP satellite orbits are nearly circular and sun-synchronous, with an altitude of 860 km and an inclination of 98.8°, and these satellites cross the equator at fixed local times.

AMSR-E is one of the six sensors aboard *Aqua*, which flies in a sun-synchronous orbit. It is a PMW radiometer, measuring brightness temperatures at 12 channels and 6 frequencies ranging from 6.9 to 89.0 GHz.

AMSU-B consists of PMW sounders aboard the *NOAA-15*, *-16*, and *-17* satellites, flying in sun-synchronous orbits at a nominal altitude of 833 km (Ferraro et al. 2000, 2005). AMSU-B sensors have five channels spanning the frequency range 89–183.3 GHz. Operating in a cross-track mode that scans 50° to either side of the nadir, the AMSU-B has a swath width of 2343 km.

b. Rainfall retrievals

1) RETRIEVALS FROM PR

As described in Iguchi et al. (2000), the PR algorithm utilizes a globally averaged drop size distribution (DSD) as the initial guess to obtain an attenuation-corrected radar reflectivity–rain rate (Ze–*R*) relationship that is consistent with the assumed DSD model. After taking attenuation correction into account, the true effective reflectivity factor Ze is first estimated at 13.8 GHz at each radar resolution cell from the measured vertical profiles of reflectivity factor. The rainfall rate *R* is then computed from the estimated Ze. Several factors, as discussed by Iguchi et al. (2000) and Masunaga et al. (2002), may affect the accuracy of the estimated rain rate, including assumptions in the DSD model, uncertainties in the attenuation correction, and corrections for nonuniform beam-filling effects. The footprint resolution of a PR rain pixel is about 5 km at nadir and the minimum detectable rain rate is about 0.3–0.5 mm h^{-1}.

2) RETRIEVALS FROM PMW SOUNDERS

Originally developed for retrieving moisture profiles, the AMSU-B capability has been expanded to operationally retrieve surface precipitation through detection of the scattering associated with precipitation-sized ice particles since 2001. The same algorithm is employed for rainfall retrievals over both land and ocean. As described in Zhao and Weng (2002), Weng et al. (2003), and Ferraro et al. (2005), the cloud ice water path (IWP) and ice particle effective diameters are first derived using the AMSU channels at 89 and 150 GHz. The derived IWP is then converted into surface rain rate through an IWP and rainfall rate relationship developed from cloud model results. Ferraro et al. (2005) compared daily AMSU-B rainfall retrievals against a composite radar–rain gauge rainfall product for a land-falling tropical cyclone over Texas and noticed that the rainfall retrieval tends to overestimate the light rainfall and underestimate the heavier amounts. Overall, AMSU-B rain retrievals have reasonably high correlations with ground-based measurements. The minimum detectable rain rate is 1.1 mm h^{-1}, and the maximum is about 30 mm h^{-1} (R. Ferraro 2006, personal communication).

3) RETRIEVALS FROM PMW IMAGERS

The microwave rainfall retrievals used for TMI, SSM/I, and AMSR-E are essentially all based on the most recent version of the National Aeronautics and Space Adninistration (NASA) Goddard Profiling (GPROF, version 6) algorithm (Kummerow et al. 1996, 2001; Olson et al. 1999, 2006). The GPROF has been designed to be portable from sensor to sensor and is widely considered as a "community consensus approach." The data provide a unique opportunity to examine the difference of rainfall estimates derived from the same algorithm but applied to PMW sensors on board different satellites. Over the ocean, the microwave frequencies can probe through smaller cloud particles to measure the microwave emission from the larger raindrops. Over land, the sensors can also measure the scattering effects of large ice particles that later melt to form raindrops. Based on the radiance contrast between the surface and raindrops at the available passive microwave channels, the GPROF algorithm physically retrieves the vertical hydrometeor profiles that best fit the observed microwave radiance. A library of hydrometer profiles generated by a cloud-resolving model is scanned to find which profiles are radiatively compatible with the observations; the retrieved profiles, including the surface rain rates, are a Bayesian composite of the compatible profiles.

c. *Definition of coincident spatially averaged observations*

The purpose of this study is to quantitatively evaluate rainfall estimates from various PMW imagers and sounders against a unified reference framework. Rainfall estimates from PR, TMI, SSM/I, AMSR-E, and AMSU-B are analyzed from January 2005 to August 2006. Because rain pixel resolutions of most PMW sensors are slightly smaller than or close to a quarter degree and global atmospheric models and analysis systems are moving toward providing forecasts and products at resolutions ranging from 0.1° to 0.5° (10–50 km), all the instantaneous rainfall pixel data are first horizontally averaged onto 0.25° × 0.25° grid boxes for each individual satellite dataset. Only those grid boxes that are entirely covered by satellite scans are further considered in coincident computations.

Because the life cycle of an individual cumulus is usually less than 1 h, and the grid box–averaged rainfall retrievals from satellites are only snapshots of a 0.25° × 0.25° grid box for a duration of less than a second, many earlier validation studies use 10–15-min intervals to define the coincidence of sensors from different platforms and evaluate single satellite retrievals against surface radar and gauge data (e.g., Ebert et al. 1996; Smith et al. 1998; Ebert and Manton 1998; Schumacher and Houze 2000; Liao et al. 2001; Yang et al. 2006). In this study, we follow the same assumption used in the earlier validation studies so that when TRMM PR and any one of the PMW sensors overpass a 0.25° × 0.25° grid box within 10 min, we consider that they are sampling the same precipitating/nonprecipitating event. Then pairs of collocated samples are collected for further statistical analyses.

Figure 1 shows accumulated coincident sample numbers of different PMW sensors versus TRMM PR over a 20-month period from January 2005 to August 2006. Because TMI and PR are on the same TRMM satellite, their ground tracks are always collocated between 35°S and 35°N. The average sample numbers are about 100 to 200 in the tropics and gradually increase toward higher latitudes. For other satellites collocated with TRMM PR, the sample numbers still indicate some gaps in lower latitudes, largely because of the strict definition of coincidence. Especially during individual months, the collocated sample numbers may be concentrated over some limited areas with other areas not being sampled at all because of the orbit. The sensitivity of the rainfall error statistics over different regions will be examined in a separate study. Nevertheless the 20-month accumulation does have a relatively even coverage in both the tropics and subtropics over different climate regimes, in contrast to the very limited overpass samples in ground-based validation studies.

By relaxing the definition of coincidence from 10 min to 20, 30, or 60 min, the collocated samples increase dramatically and can fully cover the entire low latitudes. Sensitivities of the coincidence assumption will be reported in later studies to further examine the impact of temporal and spatial resolutions on rain detection and retrieval error statistics.

3. Rain detection

Successful simulations of rain frequency and rain intensity at high temporal and spatial resolutions represent key metrics for testing the influence of model physical parameterizations on the hydrological cycle. As an important resource of observational dataset, satellite rain retrievals, however, may have significantly large differences in rain incidence and probability density function of raining events because of sensors' and algorithms' technical detection capabilities and the employment of various rain–no rain screening techniques (Grody 1991; Ebert et al. 1996; Smith et al. 1998; Ferraro et al. 1998). Such problems in rain pixel identification become especially severe over highly variable surface backgrounds and/or when examining light-rain events; this will be an important issue to be improved in future satellite missions.

In this study, instead of examining the discrepancies of rain detection capabilities at the pixel level, we evaluate the area-averaged rain rate at a 0.25° × 0.25° resolution so that different retrievals can be meaningfully compared at the same resolution. Similar to those calculations performed by Kummerow et al. (2001) and Chen and Staelin (2003) using ground-based measurements, all the collocated rain retrievals (including both zero and nonzero rain rates) are stratified into four groups: (i) both PR and PMW sensor rain rates = 0, (ii) both PR and PMW sensor rain rates > 0, (iii) PR rain rate > 0 but the sensor rain rate = 0, and (iv) PR rain rate = 0 but the sensor rain rate > 0.

Figure 2 shows the percentage of incidence of these four groups relative to the total coincident samples over the ocean between 35°S and 35°N (the TRMM ocean domain, hereinafter referred to as TRMM Ocean). As expected, the situation when retrievals from both PR and individual PMW sensors indicate zero rain rates dominates the coincident samples (ranging from 82% to 85%), with TMI and AMSR-E at the low end, SSM/I in the middle, and AMSU-B at the high end. The imager and sounder data indicate large differences in the situation when retrievals from both PR and PMW sensors indicate above-zero rain rates: there are about 8%

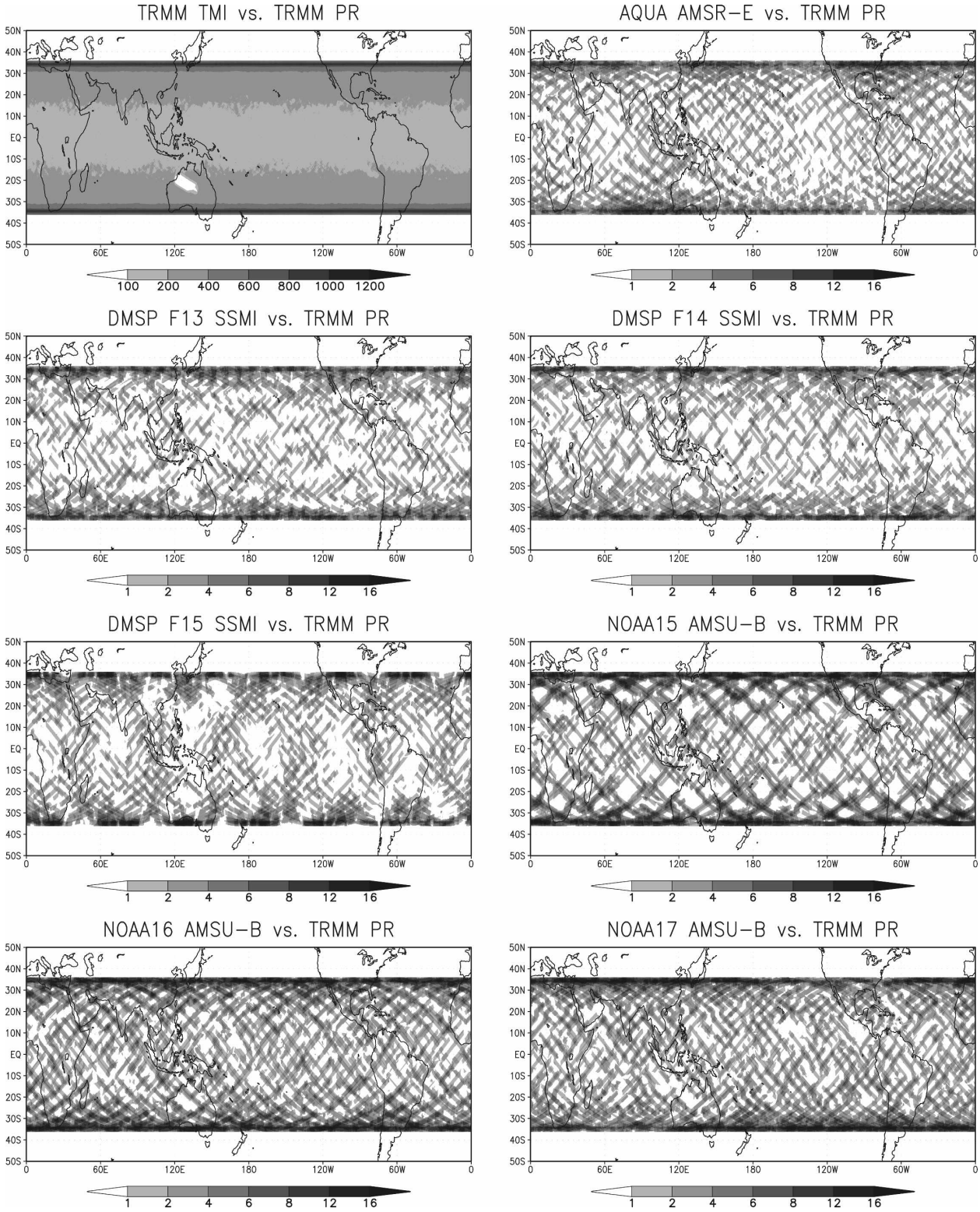

FIG. 1. Sample numbers collocated with TRMM PR (0.25° × 0.25°, 10-min intervals) for TRMM TMI, *Aqua* AMSR-E, SSM/I from the DMSP *F-13*, *-14*, and *-15* satellites, and AMSU-B from *NOAA-15*, *-16*, and *-17* satellites for a 20-month period from January 2005 to August 2006.

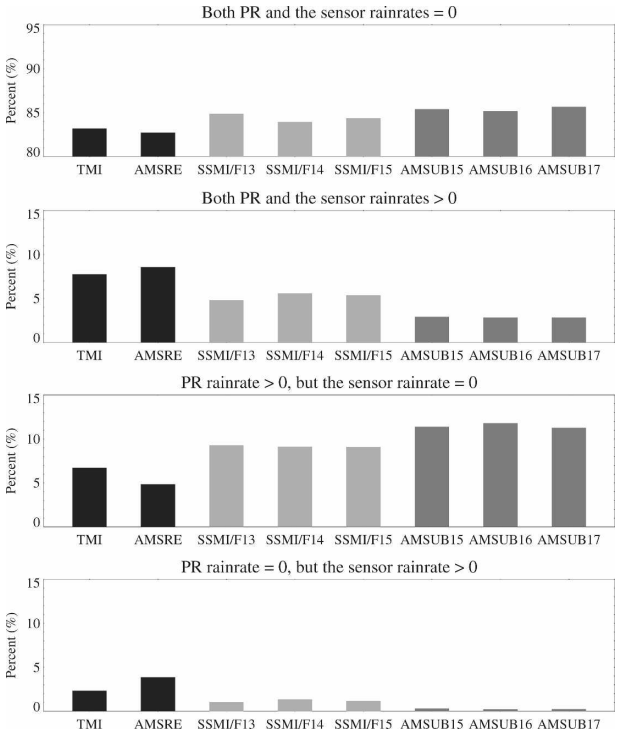

FIG. 2. The percentage of occurrence of four collocated rain–no rain situations relative to the total coincident samples over the TRMM Ocean: (top to bottom) both PR and PMW sensor rain rates = 0, both PR and PMW sensor rain rates > 0, PR rain rate > 0 but individual PMW sensor rain rate = 0, and PR rain rate = 0 but individual PMW sensor rain rate > 0.

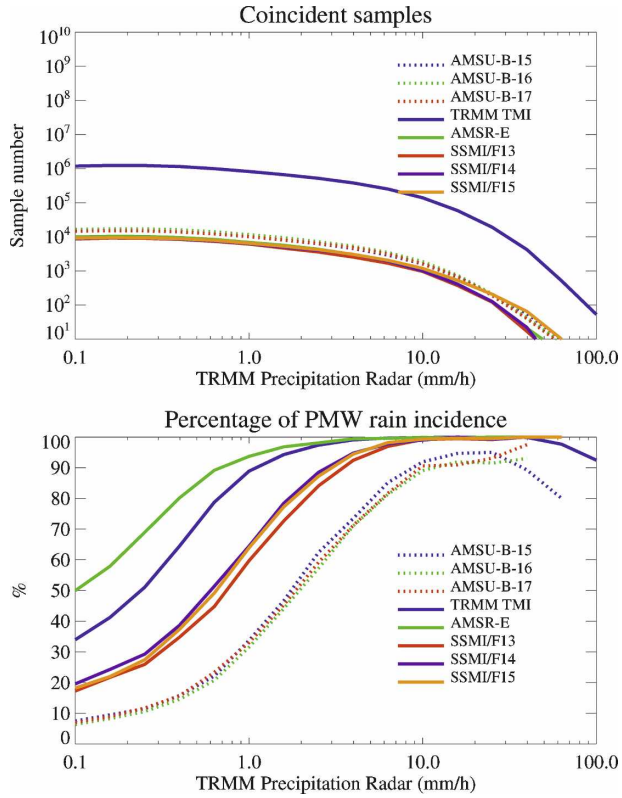

FIG. 3. (top) Coincident sample numbers and (bottom) percentage of zero rain rates (at 0.25° × 0.25° resolution) from the PMW imager and sounder relative to TRMM PR data over the TRMM Ocean from January 2005 to August 2006.

of coincident samples in which TMI and AMSR-E indicate rain incidence when PR does. SSM/I retrievals, although employing the same GPROF 6 algorithm, have only about 5% of coincident samples showing nonzero rain simultaneously. Retrievals from AMSU-B, however, indicate the lowest frequency of occurrence (slightly above 2%).

Large discrepancies can also be noticed in the situation when PR can detect rain but individual PMW sensors cannot. Among different PMW retrievals, more than 10% of AMSU-B total coincident samples cannot detect any rain over ocean when PR sees rain at the same time. The frequency of occurrence for the sounder data is about 2%–3% higher than those for SSM/I and is almost twice as much as those for TMI and AMSR-E. Joyce et al. (2004), in developing a methodology to produce a high-resolution global precipitation product, compared SSM/I and AMSU-B retrievals against TMI rainfall estimates. They attributed the small difference between SSM/I and TMI to the different retrieval footprint resolutions resulting from satellite altitudes; the large difference between AMSU-B and TMI is mainly associated with AMSU-B's high-frequency-only channels that cannot detect liquid-phase hydrometeors over ocean. Huffman et al. (2007), in calibrating different PMW retrievals using TMI data, also noticed that the AMSU-B fractional occurrence of precipitation in the subtropical oceans where light-rain events frequently occur is notably deficient relative to TMI. Considering that the situation in which PR indicates no rain but individual PMW sensors suggest nonzero rain occurs infrequently especially for SSM/I and AMSU-B retrievals, most of the above discrepancies among PMW rainfall estimates support earlier findings that over tropical and subtropical oceans, the sounder data, not being able to detect emission signatures of liquid-phase hydrometeors, have less sensible detection capabilities than the imager data.

By dividing the collocated PR rain estimates into different rain intensity bins, we can further examine the corresponding PMW detection capability as a function of PR rain intensities. Displayed in Fig. 3 are coincident sample numbers and percentages of PMW rain incidence for different PR rain intensity bins. Except for TMI, which is always collocated with PR, the binned coincident sample numbers for other satellites are simi-

lar and range between 100 and 10 000 for rain rates <30 mm h^{-1}, large enough for meaningful statistical computations. Above 30 mm h^{-1}, sample numbers for each rain intensity bin range from 10 to 100 and caution should be taken when examining the statistical results.

All the PMW sensors indicate improved detection capabilities as PR rain intensity becomes larger. AMSR-E and TMI overall compare better to PR than SSM/I and AMSU-B do, and percentages of rain incidence increase from 50% at 0.1 mm h^{-1} to 93% at 1.0 mm h^{-1} for AMSR-E and from 35% at 0.1 mm h^{-1} to 90% at 1.0 mm h^{-1} for TMI. Neither SSM/I nor AMSU-B compares well to PR at light-rain rate ranges, but SSM/I generally performs better than AMSU-B, with the percentage of rain incidence around 55% at 1.0 mm h^{-1}. On the other hand, not being able to detect liquid-phase hydrometeors over ocean, AMSU-B tends to miss most of the light-rain events, with the percentage of rain incidence around 7% at 0.1 mm h^{-1} and 25% at 1.0 mm h^{-1}. One interesting thing to note is that when the PR rain intensity is above 10 mm h^{-1}, all imager data can detect rain incidence as PR does, but there are still 6%–10% of AMSU-B coincident samples that fail to detect any rain even though PR suggests such high rain intensities. This discrepancy could probably result from heavy precipitating events that do not involve ice microphysical processes.

Although it is arguable which retrievals are better over ocean, the retrievals from the imager data (especially TMI and AMSR-E) or the PR estimates, PR data are generally considered to outperform PMW retrievals over land. The difficulties in distinguishing small radiance contrasts between rainfall and the land surface based on the scattering-only signatures have made PMW rainfall estimations over land a very challenging work. Very limited cloud simulation samples over land, together with highly variable land surface (e.g., wetness, vegetation coverage, seasonal changes) which involves many screening techniques, further complicate the problem (e.g., Grody 1991; Adler et al. 1994; Ferraro et al. 1998; Kummerow et al. 2001). Over the TRMM land area between 35°N and 35°S (hereinafter referred to as TRMM Land; Fig. 4), the situation in which both PR and PMW retrievals indicate zero rain rates again dominates the total coincident samples (about 85%–90%). The incidence when both PR and PMW retrieval indicate above-zero rain rates is about 3%–5%, with retrievals from AMSU-B indicating a slightly higher frequency of occurrence. The most prominent feature is that the PMW retrievals from both the imager and sounder data tend to have similar incidence for the situation in which PR suggests rain but individual PMW sensors do not. AMSU-B data even

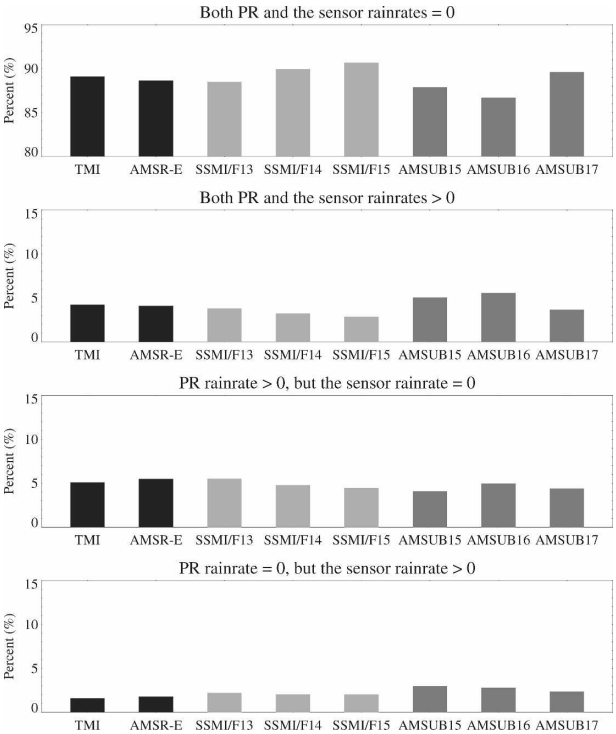

FIG. 4. As in Fig. 2, but relative to the total coincident samples over the TRMM Land.

indicate a slightly higher frequency of occurrence (1%–2% higher) relative to the imager data when PMW sensors indicate rain but PR does not.

Figure 5 further shows the coincident sample numbers and percentages of PMW rain incidence for different PR rain intensity bins over the TRMM Land. Again, the binned coincident sample number for each satellite is large enough for meaningful statistical analysis. All the passive microwave retrievals generally indicate similar detection capabilities over land. But there are subtle differences: below 1.0 mm h^{-1}, the sounder data overall agree better with the PR data than the imager data do in terms of rain incidence, whereas above 1.0 mm h^{-1}, the sounder data appear to perform equally well with TMI and AMSR-E and are in general better than SSM/I.

Because the rain retrieval algorithms have significantly different features over land and ocean, in the follow sections we evaluate their frequency distribution functions and rain error statistics over TRMM Ocean and TRMM Land separately.

4. Coincident comparisons with PR over TRMM Ocean

Many earlier studies have evaluated PMW rainfall retrievals from individual sensors on board single sat-

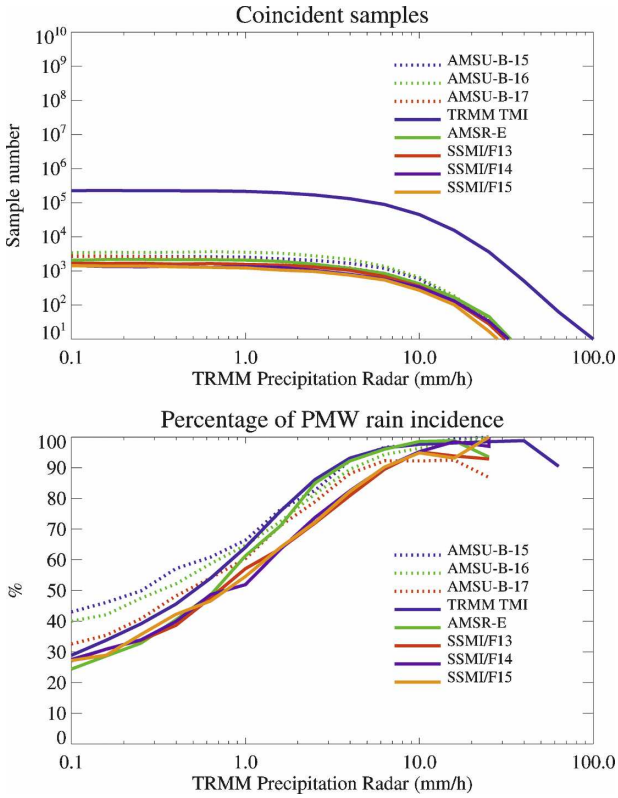

FIG. 5. As in Fig. 3, but for TRMM Land.

ellites over tropical and subtropical oceans. Here we compare several instantaneous PMW rainfall retrievals from imagers and sounders on board different satellites with PR data over ocean. Figure 6 shows the conventional scatterplot between collocated rain retrievals from TRMM PR and individual PMW sensors over TRMM Ocean for August 2005. Similar to what has been noticed in earlier studies, the coincident rain samples are dominated by samples with rain intensities below 10 mm h^{-1}. Although some underestimations can be noted at very high intensities, TMI retrievals appear to agree pretty well with PR at all high, intermediate, and low rain intensities. This is consistent with in the findings of Yang et al. (2006), namely, that different GPROF versions of TMI rainfall retrievals at instantaneous 0.5° resolution have high correlations with coincident PR estimates over tropical and subtropical oceans. Rain estimations from AMSR-E, SSM/I, and AMSU-B also correlate nicely at high and intermediate rain intensities. However, close to and below a rain intensity of 1 mm h^{-1} (which is about the cutoff rate at these retrievals' pixel level), both SSM/I and AMSU-B retrievals appear to indicate slightly higher intensities than their coincident PR data and tend to set their rain rates around the cutoff rates for many situations in which PR rain rates are below 1 mm h^{-1}. Considering what is shown in Fig. 3 (i.e., that SSM/I and AMSU-B tend to have much lower detection capabilities than TMI and AMSR-E), we hypothesize that such discrepancies in rain incidence and scatterplot are primarily associated with the difference in sensitivity and detection capability among PMW sensors in light-rain events. SSM/I and AMSU-B tend either to retrieve no-rain situations or to bias toward higher rain rates (the beamfilling problem), whereas TMI and AMSR-E have better sensitivities in light-rain cases because of the inclusion of information from better resolutions, more emission channels, and careful calibrations with TRMM PR data.

To further illustrate the impact of detection capabilities as a function of PR rain intensities among various PMW retrievals, probability density functions (PDFs) of collocated raining samples over the TRMM Ocean are shown in Fig. 7. Consistent with earlier studies (e.g., Kummerow et al. 2001; Joyce et al. 2004; Nesbitt et al. 2004), PR data indicate that a large portion of raining samples consists of light-rain events. The frequency of rain occurrence from both TMI and AMSR-E agree pretty well with PR data above 1 mm h^{-1}, with some small underestimations below 1 mm h^{-1}. AMSR-E estimates appear to be even slightly better than TMI. The three SSM/I datasets tend to underestimate PR more than TMI and AMSR-E do in term of the frequency of light-rain events and to overestimate PR in the range between 1.5 and 6.0 mm h^{-1}. Rain retrievals from AMSU-B appear to need some more improvement over the tropical and subtropical ocean. Most of the light-rain events are not sufficiently detected because AMSU-B is less capable of detecting the prevalent precipitation from warm-topped clouds (Petty 1999; Joyce et al. 2004; Huffman et al. 2007). Similar to what shown in the SSM/I plots, rain events at intermediate rain intensities (ranging between 2.0 and 10.0 mm h^{-1}, higher that those shown in SSM/I) are overly sampled by AMSU-B. These underestimations of the frequency of light-rain events and overestimations of the frequency of intermediate-rain events in SSM/I and AMSU-B retrievals, also noted in Joyce et al. (2004), are probably manifestations of the misrepresentation of light-rain events by these PMW sensors: they could detect too many no-rain situations and/or sometimes overestimate the light-rain intensity, thus aliasing errors into intermediate rain rate ranges.

Because statistical measures could be easily weighted toward raining samples that occur the most frequently (Conner and Petty 1998), namely, the light-rain events, rain error statistics have long been recognized as a

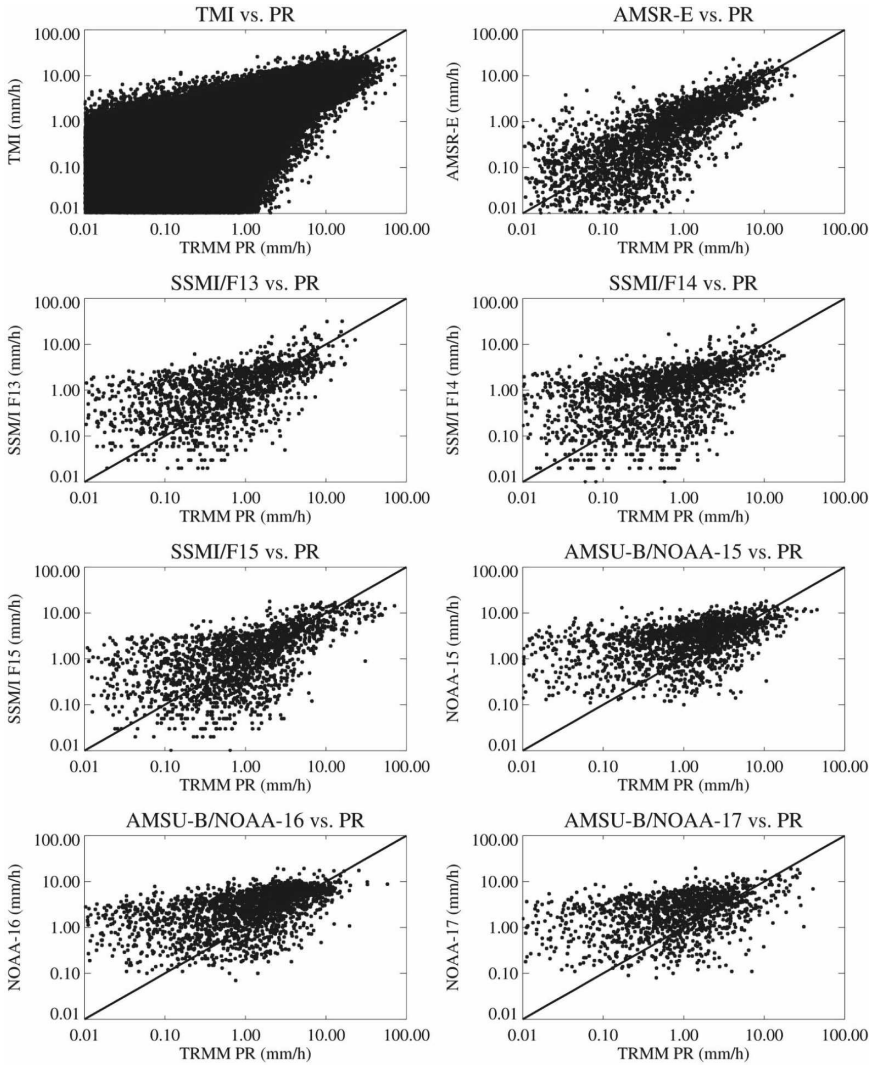

FIG. 6. Scatterplots of collocated rain rates from TRMM PR and individual PMW sensors over the TRMM Ocean for August 2005.

strong function of rain intensity. A number of studies have examined single PMW rainfall retrievals against PR or ground validation data at different rain intensities (e.g., Chen and Staelin 2003; Olson et al. 2006); however, the rain error statistics among various PMW retrievals on board different satellites have not been thoroughly compared. In this study, by grouping a tremendous amount of coincident PR rain retrievals into rain intensity bins, systematic biases, root-mean-square (RMS) errors, and standard deviation (STD) errors can be evaluated for various PMW retrievals against the same reference framework. Such error statistics are also very useful for assimilating different satellite rainfall retrievals into numerical weather prediction models. For each individual PR rain intensity bin, the coincident retrievals from PMW sensors can be any valid value, including both zero and nonzero rain rates.

Figure 8 shows the normalized systematic biases and RMS errors in percentage for collocated PR rain intensities (at a $0.25° \times 0.25°$ resolution) from January 2005 to August 2006 over ocean areas sampled by TRMM. Areas with rain intensity <1.0 mm h^{-1}, representing the largest minimum detectable rain rate for these PMW sensors, are lightly shaded. Rain retrievals from both imager and sounder data perform very well between 0.3 and 10 mm h^{-1} and the largest systematic bias is smaller than 20%. There is a negative bias in high-rain intensity ranges (above 10 mm h^{-1}) for all PMW retrievals. The amplitude of the negative bias tends to become larger as the rain intensity increases, and the

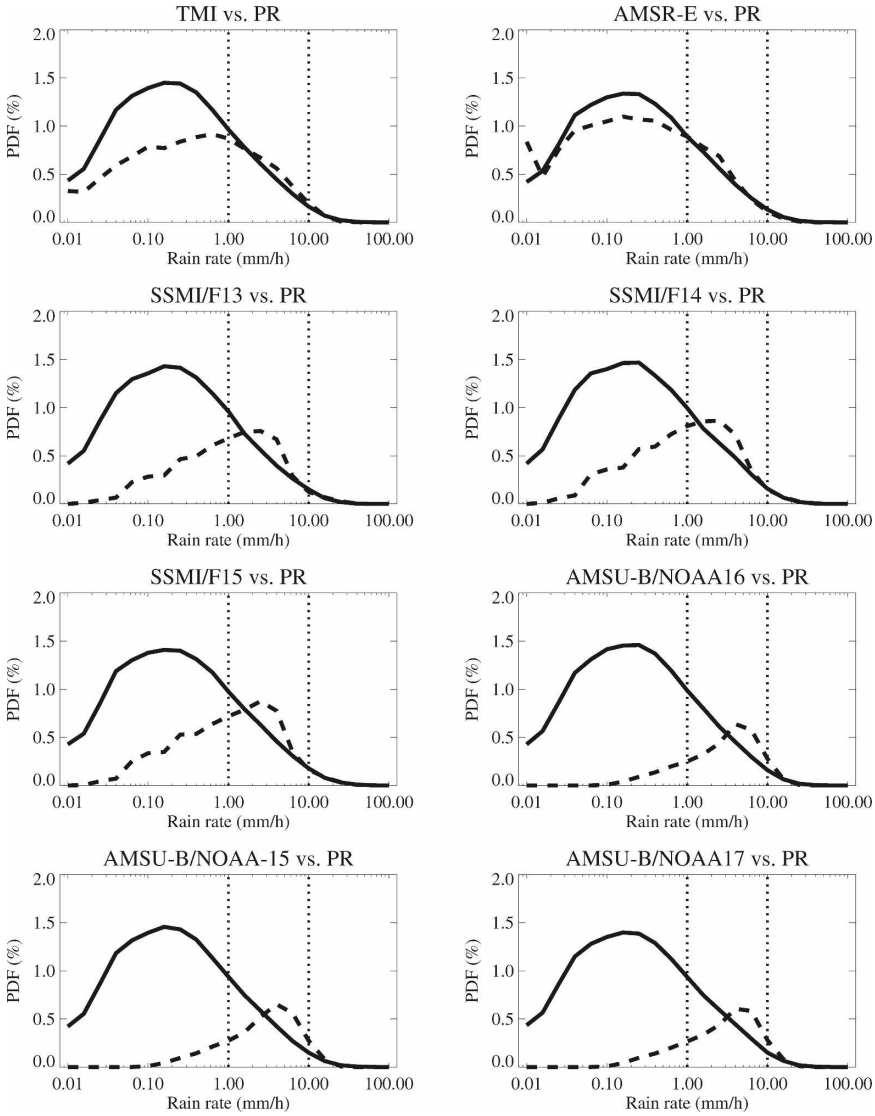

FIG. 7. PDFs of collocated rain rates at 0.25° × 0.25° resolutions (PR: solid line; PMW sensors: thick dashed line) over the TRMM Ocean for a period of 20 months from January 2005 to August 2006. The thin dotted vertical lines represent rain rates of (left) 1.0 and (right) 10.0 mm h^{-1}.

sounder data appear to have larger negative biases than the imager data. Below 0.3 mm h^{-1}, TMI and AMSR-E retrievals have smaller biases than retrievals from SSM/I and AMSU-B. There are large positive biases below 0.3 mm h^{-1} for SSM/I and AMSU-B retrievals, and the normalized bias increases with reducing rain intensities. These positive biases, as discussed earlier, are possibly associated with the frequent misrepresentation of light rain as intermediate-rain pixels in SSM/I and AMSU-B algorithms.

All the PMW rainfall retrievals indicate that their normalized RMS errors tend to have an inverse relationship with the TRMM PR rain rate, so that relative errors become much larger in light-rain events and smaller in heavy-rain events. These features have been noticed in many earlier studies over both oceanic and land areas (e.g., Bell and Reid 1993; Huffman 1997; Olson et al. 2006). For heavy-rain events (above 10 mm h^{-1}), all the algorithms perform pretty well over the TRMM Ocean. The largest relative RMS errors, at a resolution of 0.25° × 0.25°, range between 50% and 70% for the imager and sounder data. Below 5.0 mm h^{-1}, however, there are significant differences in the relative RMS error among these PMW retrievals. Both TMI and AMSR-E retrievals continue to outperform SSM/I retrievals from three DMSP satellites and

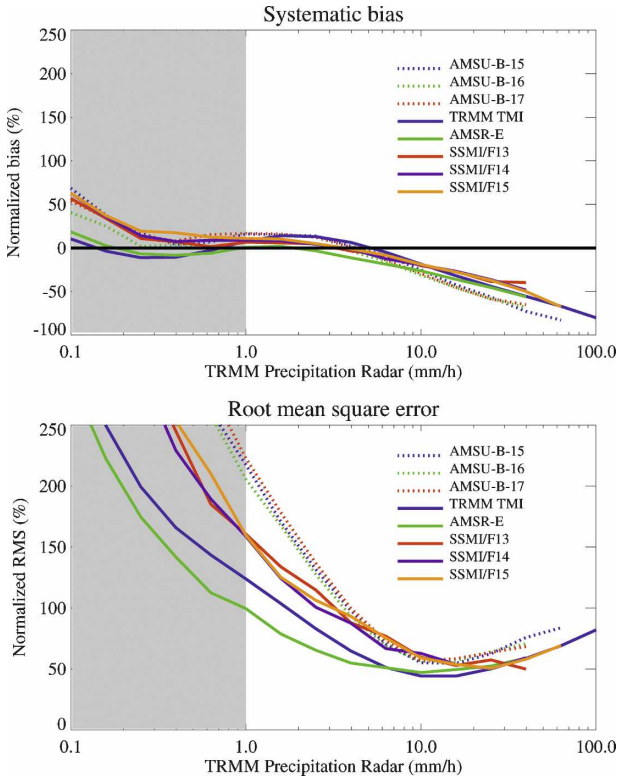

FIG. 8. (top) Normalized biases and (bottom) RMS errors of rain retrievals (at 0.25° × 0.25° resolution) from the PMW imager and sounder relative to TRMM PR data over the TRMM Ocean from January 2005 to August 2006. The area of rain intensity <1.0 mm h^{-1} is lightly shaded.

AMSU-B retrievals from three NOAA satellites, with the RMS error close to 100%–120% at a rain intensity of 1.0 mm h^{-1}. AMSU-B retrievals, although from different NOAA sun-synchronous satellites, agree with one another and have the largest RMS error relative to AMSR-E, TMI, and SSM/I. The relative RMS error is around 230% at a rain intensity of 1.0 mm h^{-1}.

Taking their minimum cutoff rain rates into account, all the PMW retrievals have similarly small systematic biases over the TRMM Ocean in comparison with PR data. For instantaneous rain rates above 10 mm h^{-1}, all the PMW retrievals also have similar RMS errors, indicating that both imager and sounder data have similar capabilities to capture heavy-rain events. For instantaneous rain rates below 5 mm h^{-1}, the imager data clearly have smaller RMS errors than the sounder data over tropical and subtropical oceans, especially in light-rain events. Part of the reason may be associated with the fact that AMSU-B rain estimates retrieve precipitation based on the relationship between surface precipitation and ice water content and thus miss the frequent and important warm-rain processes in the tropics and subtropics (Petty 1999; Joyce et al. 2004; Huffman et al. 2007).

5. Coincident comparisons with TRMM PR over land

It is well known that rain retrievals by PMW sensors are less reliable over land than those over ocean because of the empirical relationship between cloud ice content and surface rain rate, as well as the difficulties in distinguishing rain pixels from nonuniform and complicated backgrounds. Improving PMW rainfall estimation accuracy over land presents an important challenge to any future satellite precipitation measuring mission. On the other hand, because PR does not need to take varying land surface into account, spaceborne PR estimations are both theoretically and practically superior to PMW retrievals over land. Displayed in Fig. 9 are scatterplots between collocated rain retrievals from TRMM PR and individual PMW sensors over the TRMM Land for August 2005. All the PMW retrievals show good agreement with TRMM PR above 1.0 mm h^{-1}, suggesting that both PR and PMW instantaneous rain retrievals can capture heavy and intermediate rain events over land reasonably well. For PR rain rates below 1.0 mm h^{-1} there is a tendency for PMW retrievals to gradually lose the linear relationship with PR data, and the PMW rainfall estimates could be anywhere between 0.1 and 4.0 mm h^{-1}. Such discrepancies again reflect limitations in detecting light-rain events by current PMW retrievals over land.

Figure 10 shows PDFs of collocated raining samples over the TRMM Land for a period of 20 months. For rain intensities below 0.5 mm h^{-1}, all the imager and sounder data indicate similar underestimations in the incidence of light-rain events. Above 0.5 mm h^{-1}, TMI and AMSR-E retrievals tend to perform the best and nearly match with TRMM PR data. SSM/I and AMSU-B retrievals, however, indicate some overestimations in rain incidence between 1.0 and 10.0 mm h^{-1}, with AMSU-B showing the largest overestimations. These overestimations, as shown in plots for TRMM Ocean, could possibly result from aliasing errors by mistakenly identifying light-rain samples as intermediate-rain samples.

The normalized systematic biases over the TRMM Land (in Fig. 11), similar to those over the TRMM Ocean, continue to show increasingly negative biases for heavy-rain samples and increasingly positive biases for light-rain samples. Ferraro et al. (2005), in comparing AMSU rainfall retrievals versus a radar–rain gauge composite rainfall product for a landfalling tropical cyclone, also noticed that AMSU retrievals tend to overestimate the light rainfall and underestimate the heavi-

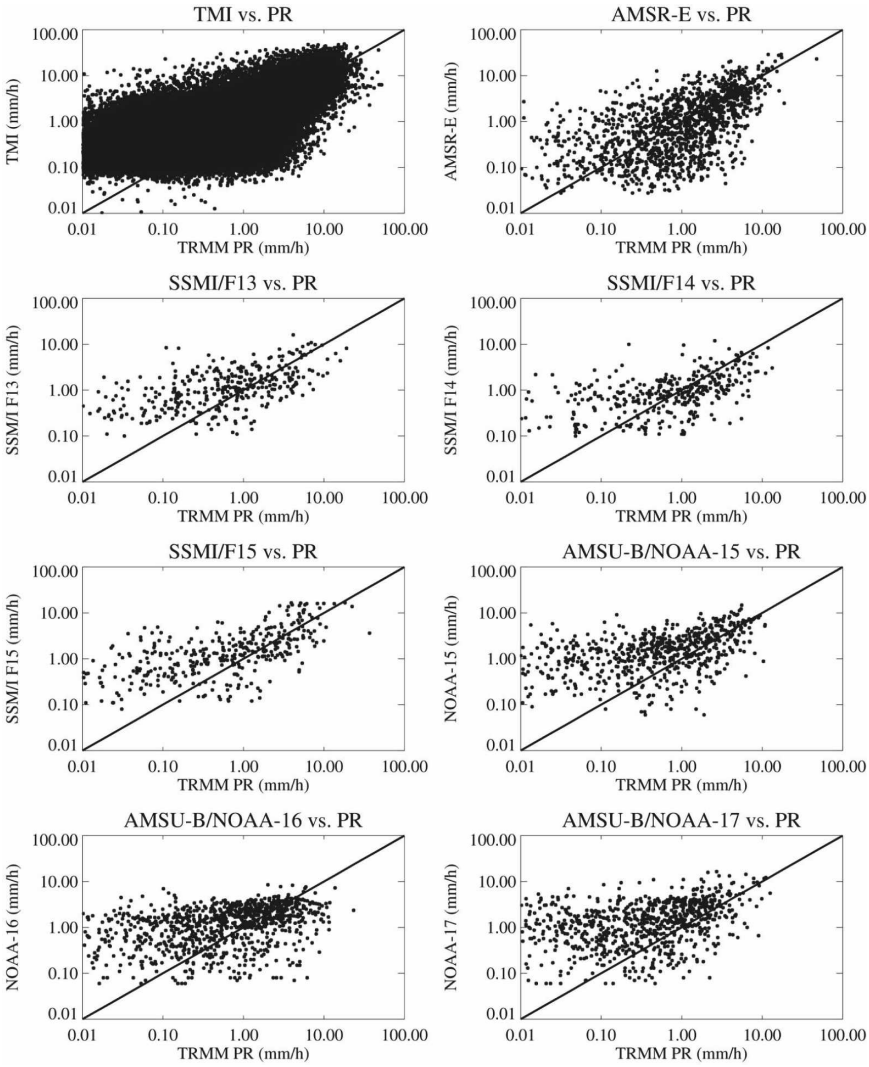

FIG. 9. As in Fig. 6, but for TRMM Land.

er rainfall. For heavy-rain samples, the amplitudes of negative biases over land and ocean are similar, with TMI and AMSR-E even indicating smaller biases over land relative to their counterparts over ocean. Among all the land algorithms, the AMSR-E retrieval overall has the smallest systematic bias, and TMI the second smallest. Both SSM/I and AMSU-B indicate a relatively large systematic bias below 2.0 mm h^{-1}, in dramatic contrast to the generally small systematic bias shown in the ocean algorithms.

The normalized RMS error plot shows that rain estimates from the sounder and imager data have comparable RMS errors over land. Although TMI and AMSR-E still indicate slightly smaller RMS errors below 1.0 mm h^{-1} than AMSU-B does, AMSU-B generally performs better than SSM/I and the overall difference between the sounder and imager data is much smaller over land than over ocean for light-rain events. Relative to SSM/I, AMSR-E, and TMI, AMSU-B data even show slightly smaller RMS errors for rain intensities above 2.0 mm h^{-1}. The average relative RMS error is between 200% and 250% when PR rain intensity is close to 1.0 mm h^{-1} and between 50% and 80% when PR rain intensity is around 10 mm h^{-1}. Therefore, even though AMSU-B data are somewhat worse than the imager data over ocean, especially for rain intensities <5 mm h^{-1}, they are in general comparable in quality to those derived from conically scanning radiometers over land for instantaneous rain rates. If this is true, then cross-track microwave sounders with high-frequency channels on operational satellites could be included in future precipitation measurement constellations to achieve better sampling and coverage over land.

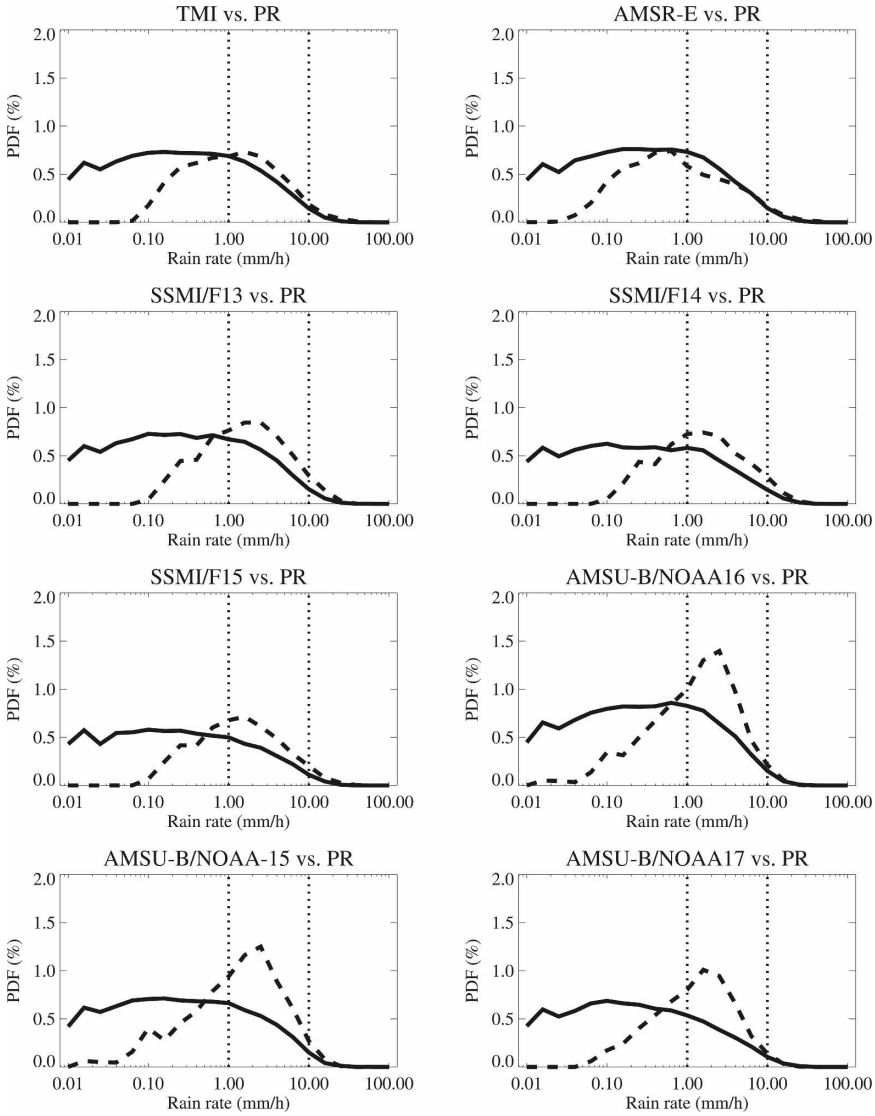

FIG. 10. As in Fig. 7, but for TRMM Land.

6. Comparisons with ground measurements over the continental United States

Although PR data are extensively used as a reference in this study to evaluate PMW imager and sounder data, they do have uncertainties and should not be treated as the truth. To further confirm the results obtained from coincident comparisons with TRMM PR over land, we have also performed similar coincident comparisons over the continental United States, using surface radar and rain gauge data as another independent reference to check the consistency of the result. Another purpose of this exercise is to demonstrate whether or not the theoretically superior TRMM PR data are indeed better than PMW rain retrievals over land. The ground validation data used in this study are the merged surface radar and rain gauge product from the National Centers for Environmental Prediction (NCEP) National Hourly Multisensor Precipitation Analysis Stage IV (Lin and Mitchell 2005). This dataset collects hourly radar rainfall estimates from about 140 Weather Surveillance Radar-1988 Doppler (WSR-88D) operational radars over the continental United States, merging with about 3000 hourly gauge reports. The stage IV data are preliminarily quality controlled and calibrated. The original precipitation product is at the 4-km resolution, and the data are horizontally averaged onto the same 0.25° × 0.25° grids as the satellite rain retrievals. Because the ground measurements are only available at 1-h intervals, the definition of coincidence

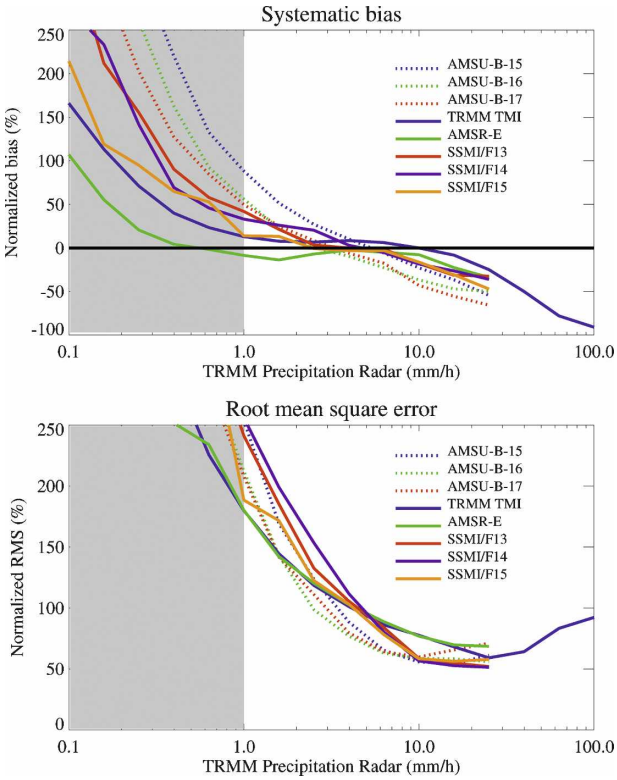

FIG. 11. As in Fig. 8, but for TRMM Land.

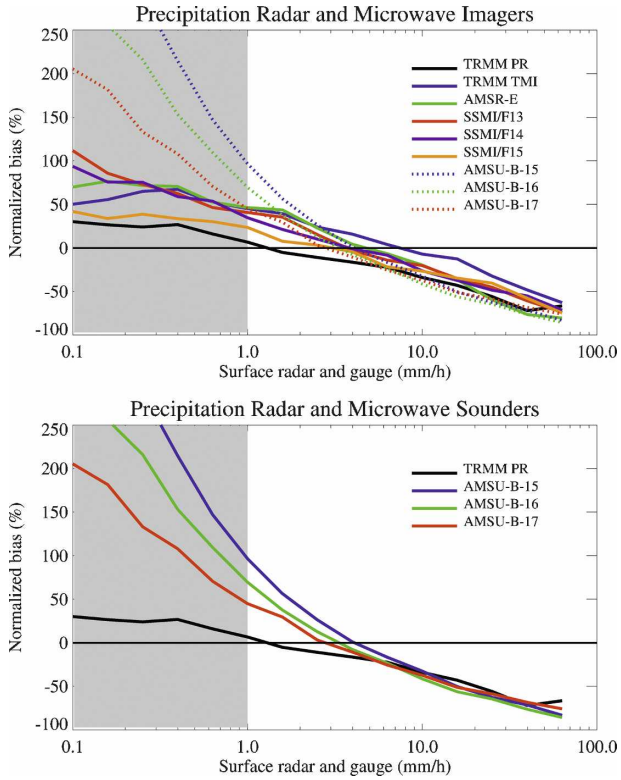

FIG. 12. Normalized bias of rain retrievals (at 0.25° × 0.25° resolution at 1-h intervals) from the TRMM PR and (top) PMW imager and (bottom) sounder relative to a merged surface radar and gauge product over the continental United States from June to August 2005. The area of rain intensity <1.0 mm h^{-1} is lightly shaded.

has to be relaxed to 1 h in this section, but the temporal variance of instantaneous rain estimates versus hourly means will be examined. The coincident comparisons are made for a 3-month period (June–August 2005) over the continental United States south of 35°N.

Figure 12 compares the normalized systematic bias of collocated rain rates from TRMM PR and PMW sensors against surface radar and gauge data. All the satellite rainfall retrievals again indicate increasingly positive biases above 10 mm h^{-1} and increasingly negative biases <5 mm h^{-1}. PR data indeed have the smallest systematic bias at light-rain and intermediate-rain intensities. Above 10 mm h^{-1}, however, PR data have systematic biases similar to those of the PMW retrievals. Rain retrievals from the sounder data have the largest systematic bias at light-rain intensities, consistent with the result using PR data as the reference. Above 3 mm h^{-1}, the sounder, imager, and PR data tend to have similar systematic biases.

Illustrated in Fig. 13 are the normalized STD errors of collocated rain rates from TRMM PR and PMW sensors against the merged surface radar and gauge product at 1-h intervals. The two black dashed lines represent the temporal variance of instantaneous rain rates compared to hourly mean rain rates based on surface radar data collected from two TRMM ground validation sites (Melbourne, Florida, and Houston, Texas, courtesy of David Wolf and Tom Bell). These idealized curves provide an estimation of the largest random STD error due to mismatches in observation times within an hourly window for perfect retrievals. Compared with all the PMW retrievals over land, PR rainfall estimations not only have the smallest systematic bias but also have the smallest STD error <5.0 mm h^{-1}, confirming the PR's theoretical superiority relative to PMW retrievals in accurately retrieving rainfall over land, especially at light- and intermediate-rain events. Above 5.0 mm h^{-1}, both PR and PMW retrievals tend to gradually approach the idealized curves as rain intensity increases, suggesting that PR and PMW instantaneous rain retrievals can provide similarly accurate rainfall estimations for heavy-rain samples. Comparisons of STD errors from the sounder and imager data again indicate that AMSU-B data indeed have smaller STD errors than SSM/I, AMSR-E, and TMI retrievals for instantaneous rain rates between 1.0 and 10.0 mm h^{-1}. Therefore, using a completely different and independent reference, we demonstrate that the AMSU-B

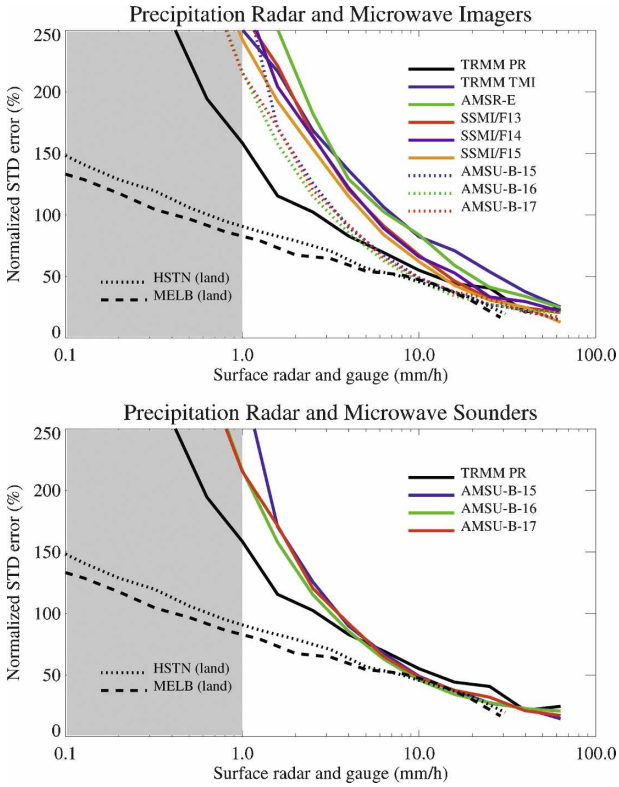

FIG. 13. As in Fig. 12, but for normalized STD. The dashes are estimations of the largest random STD errors due to mismatches in simulated satellite observation times within an hourly window for perfect retrievals based on from surface rainfall data at Houston and Melbourne (Florida) sites.

data are comparable in quality to those derived from conically scanning radiometers over land. In addition, TRMM PR data are indeed found to be superior to PMW rainfall estimations over land for rain intensities below roughly 5 mm h^{-1}. For heavy-rain events, PR data appear to perform equally well to the rainfall retrievals from the sounder and imager data.

7. Summary and conclusions

This study examines instantaneous rainfall estimates provided by the current generation of retrieval algorithms for PMW instruments using retrievals from the TRMM PR and merged surface radar/gauge measurements over the continental United States as references. The PMW sensors included in the comparison are three operational sounders (AMSU-B instruments on *NOAA-15*, *-16*, and *-17* satellites) and five imagers (TRMM TMI; SSM/I instruments on DMSP *F-13*, *-14*, and *-15* satellites; and AMSR-E on *Aqua*). The purpose is to quantitatively assess surface rain retrievals from cross-track scanning microwave humidity sounders relative to those from conically scanning microwave imagers. Coincident comparisons are conducted against TRMM PR by averaging instantaneous rainfall retrievals onto a 0.25° × 0.25° grid at 10-min intervals over a 20-month period from January 2005 to August 2006. Rain detection capabilities and retrieval error statistics are computed as a function of rain intensity over land and ocean. Additional coincident comparisons are also made against ground radar and gauge data over the continental United States at 1-h intervals over a 3-month period from June 2005 to August 2005.

Comparisons of systematic errors and RMS errors indicate that AMSU-B sounder rain estimates are comparable in quality to those from conically scanning radiometers for instantaneous rain rates between 1.0 and 10.0 mm h^{-1}. This result holds true for comparisons using either TRMM PR estimates over tropical land areas or merged ground radar–gauge measurements over the continental United States as the reference.

Over tropical and subtropical land, the sounder and imager data have similar detection capabilities, with the sounder data showing slightly better detection capabilities than the imager data. Although SSM/I and AMSU-B display a relatively larger systematic bias than TMI and AMSR-E <2.0 mm h^{-1}, all the PMW retrievals show similar incidence of light-rain events.

Over the tropical and subtropical ocean, the radiometer data generally have better detection capabilities than the sounder data, especially for light-rain events. Among the radiometer data, SSM/I has slightly worse detection capabilities than TMI and AMSR-E, largely due to the SSM/I's coarser retrieval footprint resolution resulting from satellite altitudes and fewer microwave low-frequency channels. The AMSU-B data, which are less capable of detecting emission signatures of liquid phase hydrometeors due to the availability of only high-frequency channels, tend to miss a lot of warm-topped precipitation events that are found to be prevalent in the tropics and subtropics (e.g., Petty 1995, 1999; Johnson et al. 1999; Lau and Wu 2003; Huffman et al. 2007). Some of these lower detection capabilities are manifested by underestimations of the frequency of light-rain events and overestimations of the frequency of intermediate-rain events, which are likely to result from aliasing errors. Significant efforts are being made to merge low-frequency emission signals on the AMSU-A instruments with the high-frequency scattering signals on the AMSU-B instruments so that information about liquid-phase hydrometeors can be better detected over tropical and subtropical oceans (Vila et al. 2007).

All the PMW retrievals have similarly small systematic biases over the tropical and subtropical ocean rela-

tive to TRMM PR data, and the largest relative systematic bias is smaller than 20%. The standard deviation errors are comparable between imager and sounder retrievals for rain intensities >5 mm h^{-1}, below which the imagers are noticeably better than the sounders.

The results of this study suggest that cross-track scanning microwave humidity sounders on operational satellites can be used to augment conically scanning microwave radiometers to provide better temporal sampling over land in planning future satellite missions, such as the Global Precipitation Measurement (GPM) mission (A. Y. Hou et al. 2007, unpublished manuscript), to provide the next generation of global precipitation measurement from space.

Acknowledgments. The TRMM PR and TMI pixel data, as well as the gridded SSM/I data, are obtained from the NASA GSFC Distributed Data Archive Center (DAAC). The AMSR-E data are from the National Ice and Snow Center DAAC. The authors extend their appreciation to George Huffman and Eric Nelkin for providing the gridded AMSU-B rainfall data, and also to Thomas Bell and David Wolff for providing estimates of sampling errors associated with mismatched observation times. Special thanks are given to two anonymous reviewers for critical and constructive comments that greatly improved the paper. This research is supported by the GPM Project at the NASA Goddard Space Flight Center in Greenbelt, MD.

REFERENCES

Adler, R. F., A. J. Negrid, P. R. Keehn, and I. M. Hakkarinen, 1993: Estimation of monthly rainfall over Japan and surrounding waters from a combination of low-orbit microwave and geosynchronous IR data. *J. Appl. Meteor.,* **32,** 335–356.

——, G. J. Huffman, and P. R. Keehn, 1994: Global tropical rain estimates from microwave-adjusted geosynchronous IR data. *Remote Sens. Rev.,* **11,** 125–152.

Allam, R., G. Holpin, P. Jackson, and G.-L. Liberti, 1993: Second Algorithm Intercomparison Project of the Global Precipitation Climatology Project (AIP-2): U.K. and Northwest Europe, February–April 1991. Pre-Workshop Rep., Satellite Image Applications Group, Met Office, 133 pp.

Arkin, P. A., 1979: The relationship between fractional coverage of high cloud and rainfall accumulations during GATE over the B-scale array. *Mon. Wea. Rev.,* **107,** 1382–1387.

——, and B. Meisner, 1987: The relationship between large-scale convective rainfall and cold cloud over the Western Hemisphere during 1982–1984. *Mon. Wea. Rev.,* **115,** 51–74.

Bell, T. L., and N. Reid, 1993: Detecting the diurnal cycle of rainfall using satellite observations. *J. Appl. Meteor.,* **32,** 311–322.

Berg, W., T. L'Ecuyer, and C. Kummerow, 2006: Rainfall climate regimes: The relationship of regional TRMM rainfall biases to the environment. *J. Appl. Meteor. Climatol.,* **45,** 434–454.

Chen, F. W., and D. H. Staelin, 2003: AIRS/AMSU/HSB precipitation estimates. *IEEE Trans. Geosci. Remote Sens.,* **41,** 410–417.

Conner, M. D., and G. W. Petty, 1998: Validation and intercomparison of SSM/I rain-rate retrieval methods over the continental United States. *J. Appl. Meteor.,* **37,** 679–700.

Ebert, E. E., and M. J. Manton, 1998: Performance of satellite rainfall estimation algorithms during TOGA-COARE. *J. Atmos. Sci.,* **55,** 1537–1557.

——, ——, P. A. Arkin, R. J. Allam, G. E. Holpin, and A. Gruber, 1996: Results from the GPCP Algorithm Intercomparison Programme. *Bull. Amer. Meteor. Soc.,* **77,** 2875–2887.

Ferraro, R. R., E. A. Smith, W. Berg, and G. J. Huffman, 1998: A screening methodology for passive microwave precipitation retrieval algorithms. *J. Atmos. Sci.,* **55,** 1583–1600.

——, F. Weng, N. C. Grody, and L. Zhao, 2000: Precipitation characteristics over land from the *NOAA-15* AMSU sensor. *Geophys. Res. Lett.,* **27,** 2669–2672.

——, and Coauthors, 2005: NOAA operational hydrological products derived from the Advanced Microwave Sounding Unit. *IEEE Trans. Geosci. Remote Sens.,* **43,** 1036–1049.

Griffith, C. G., W. L. Woodley, P. G. Grube, D. W. Martin, J. Stout, and D. N. Sikdar, 1978: Rain estimation from geosynchronous satellite imagery—Visible and infrared studies. *Mon. Wea. Rev.,* **106,** 1153–1171.

Grody, N. C., 1991: Classification of snow cover and precipitation using the Special Sensor Microwave/Imager (SSM/I). *J. Geophys. Res.,* **96,** 7423–7435.

Hong, Y., T. T. Wilheit, and W. R. Russell, 1997: Estimation of monthly rainfall over oceans from truncated rain-rate samples: Application to SSM/I data. *J. Atmos. Oceanic Technol.,* **14,** 1012–1022.

Huffman, G. J., 1997: Estimates of root-mean-square random error for finite samples of estimated precipitation. *J. Appl. Meteor.,* **36,** 1191–1201.

——, and Coauthors, 2007: The TRMM Multi-satellite Precipitation Analysis (TMPA): Quasi-global, multiyear, combined-sensor precipitation estimates at fine scales. *J. Hydrometeor.,* **8,** 38–55.

Iguchi, T., T. Kozu, R. Meneghini, J. Awaka, and K. Okamoto, 2000: Rain-profiling algorithm for the TRMM precipitation radar. *J. Appl. Meteor.,* **39,** 2038–2052.

Johnson, R. H., T. M. Rickenbach, S. A. Rutledge, P. E. Ciesielski, and W. H. Schubert, 1999: Trimodal characteristics of tropical convection. *J. Climate,* **12,** 2397–2418.

Joyce, R. J., J. E. Janowiak, P. A. Arkin, and P. Xie, 2004: CMORPH: A method that produces global precipitation estimates from passive microwave and infrared data at high spatial and temporal resolution. *J. Hydrometeor.,* **5,** 487–503.

Kilonsky, B. J., and C. S. Ramage, 1976: A technique for estimating tropical open-ocean rainfall from satellite observations. *J. Appl. Meteor.,* **15,** 972–975.

Kummerow, C., W. S. Olson, and L. Giglio, 1996: A simplified scheme for obtaining precipitation and vertical hydrometeor profiles from passive microwave sensors. *IEEE Trans. Geosci. Remote Sens.,* **34,** 1213–1232.

——, W. Barnes, T. Kozu, J. Shiue, and J. Simpson, 1998: The Tropical Rainfall Measuring Mission (TRMM) sensor package. *J. Atmos. Oceanic Technol.,* **15,** 809–817.

——, and Coauthors, 2000: The status of the Tropical Rainfall Measuring Mission (TRMM) after two years in orbit. *J. Appl. Meteor.,* **39,** 1965–1982.

——, and Coauthors, 2001: The evolution of the Goddard profil-

ing algorithm (GPROF) for rainfall estimation from passive microwave sensors. *J. Appl. Meteor.,* **40,** 1801–1820.

Lau, K. M., and H. T. Wu, 2003: Warm rain processes over tropical oceans and climate implications. *Geophys. Res. Lett.,* **30,** 2290, doi:10.1029/2003GL018567.

Liao, L., R. Meneghini, and T. Iguchi, 2001: Comparisons of rain rate and reflectivity factor derived from the TRMM precipitation radar and the WSR-88D over the Melbourne, Florida, site. *J. Atmos. Oceanic Technol.,* **18,** 1959–1974.

Lin, X., L. D. Fowler, and D. A. Ranfall, 2002: Flying the TRMM satellite in a general circulation model. *J. Geophys. Res.,* **107,** 4281, doi:10.1029/2001JD000619.

Lin, Y., and K. E. Mitchell, 2005: The NCEP stage II/IV hourly precipitation analyses: Development and applications. Preprints, *19th Conf. on Hydrology,* San Diego, CA, Amer. Meteor. Soc., 1.2. [Available online at http://ams.confex.com/ams/pdfpapers/83847.pdf.]

Liu, G., and J. A. Curry, 1992: Retrieval of precipitation from satellite microwave measurement using both emission and scattering. *J. Geophys. Res.,* **97,** 9959–9974.

Masunaga, H., T. Iguchi, R. Oki, and M. Kachi, 2002: Comparison of rainfall products derived from TRMM Microwave Imager and precipitation radar. *J. Appl. Meteor.,* **41,** 849–862.

Meneghini, R., and T. Kozu, 1990: *Spaceborne Weather Radar.* Artech House, 199 pp.

Nesbitt, S. W., E. J. Zipser, and C. Kummerow, 2004: An examination of version-5 rainfall estimates from the TRMM Microwave Imager, precipitation radar, and rain gauges on global, regional, and storm scales. *J. Appl. Meteor.,* **43,** 1016–1036.

Olson, W. S., C. Kummerow, G. M. Heymsfield, and L. Giglio, 1996: A method for combined passive–active microwave retrievals of cloud and precipitation profiles. *J. Appl. Meteor.,* **35,** 1763–1789.

——, ——, Y. Hong, and W.-K. Tao, 1999: Atmospheric latent heating distributions in the tropics derived from satellite passive microwave radiometer measurements. *J. Appl. Meteor.,* **38,** 633–664.

——, and Coauthors, 2006: Precipitation and latent heating distributions from satellite passive microwave radiometry. Part I: Improved method and uncertainties. *J. Appl. Meteor. Climatol.,* **45,** 702–720.

Petty, G. W., 1994a: Physical retrievals of over-ocean rain rate from multichannel microwave imaging. Part I: Theoretical characteristics of normalized polarization and scattering indices. *Meteor. Atmos. Phys.,* **54,** 79–100.

——, 1994b: Physical retrievals of over-ocean rain rate from multichannel microwave imaging. Part II: Algorithm implementation. *Meteor. Atmos. Phys.,* **54,** 101–122.

——, 1995: Frequencies and characteristics of global oceanic precipitation from shipboard present-weather reports. *Bull. Amer. Meteor. Soc.,* **76,** 1593–1616.

——, 1999: Prevalence of precipitation from warm-topped clouds over eastern Asia and the western Pacific. *J. Climate,* **12,** 220–229.

Schumacher, C., and R. A. Houze, 2000: Comparison of radar data from the TRMM satellite and Kwajalein oceanic validation site. *J. Appl. Meteor.,* **39,** 2151–2164.

Simpson, J., R. F. Adler, and G. R. North, 1988: A proposed Tropical Rainfall Measuring Mission (TRMM) satellite. *Bull. Amer. Meteor. Soc.,* **69,** 278–295.

——, C. Kummerow, W.-K. Tao, and R. F. Adler, 1996: On the Tropical Rainfall Measuring Mission (TRMM). *Meteor. Atmos. Phys.,* **60,** 19–36.

Smith, E. A., C. Kummerow, and A. Mugnai, 1994a: The emergence of inversion-type precipitation profile algorithms for estimation of precipitation from satellite microwave measurements. *Remote Sens. Rev.,* **11,** 211–242.

——, X. Xiang, A. Mugnai, R. Hood, and R. W. Spencer, 1994b: Behavior of an inversion-based precipitation retrieval algorithm with high-resolution AMPR measurements including a low-frequency 10.7-GHz channel. *J. Atmos. Oceanic Technol.,* **11,** 858–873.

——, ——, ——, and G. J. Tripoli, 1994c: Design of an inversion-based precipitation profile retrieval algorithm using an explicit cloud model for initial guess microphysics. *Meteor. Atmos. Phys.,* **54,** 53–78.

——, and Coauthors, 1998: Results of WetNet PIP-2 Project. *J. Atmos. Sci.,* **55,** 1483–1536.

Spencer, R. W., 1986: A satellite passive 37-GHz scattering-based method for measuring oceanic rain rates. *J. Climate Appl. Meteor.,* **25,** 754–766.

——, W. S. Olson, W. Rongzhang, D. W. Martin, J. A. Weinman, and D. A. Santek, 1983: Heavy thunderstorms observed over land by the *Nimbus 7* Scanning Multichannel Microwave Radiometer. *J. Climate Appl. Meteor.,* **22,** 1041–1046.

——, H. M. Goodman, and R. E. Hood, 1989: Precipitation retrieval over land and ocean with the SSM/I. Part I: Identification and characteristics of the scattering signal. *J. Atmos. Oceanic Technol.,* **6,** 254–273.

Vila, D., R. Ferraro, and R. Joyce, 2007: Evaluation and improvement of AMSU precipitation retrievals. *J. Geophys. Res.,* **112,** D20119, doi:10.1029/2007JD008617.

Weng, F., L. Zhao, R. Ferraro, G. Poe, X. Li, and N. Grody, 2003: Advanced microwave sounding unit cloud and precipitation algorithms. *Radio Sci.,* **38,** 8068, doi:10.1029/2002RS002679.

Wilheit, T. T., 1986: Some comments on passive microwave measurement of rain. *Bull. Amer. Meteor. Soc.,* **67,** 1226–1232.

——, A. T. C. Chang, S. C. V. Rao, E. B. Rodgers, and J. S. Theon, 1977: A satellite technique for quantitatively mapping rainfall rates over the oceans. *J. Appl. Meteor.,* **16,** 551–560.

Yang, S., W. S. Olson, J.-J. Wang, T. L. Bell, E. A. Smith, and C. D. Kummerow, 2006: Precipitation and latent heating distributions from satellite passive microwave radiometry. Part II: Evaluation of estimates using independent data. *J. Appl. Meteor. Climatol.,* **45,** 721–739.

Zhao, L., and F. Weng, 2002: Retrieval of ice cloud parameters using the Advanced Microwave Sounding Unit. *J. Appl. Meteor.,* **41,** 384–395.